REPORT SERIES IN AEROSOL SCIENCE
N:o 210 (2018)

Sources, sinks and transformation of BVOCs and aerosols in boreal forest boundary layer

Putian Zhou

Institute for Atmospheric and Earth System Research/Physics, Faculty of Science
University of Helsinki
Helsinki, Finland

Academic dissertation

To be presented, with the permission of the Faculty of Science of the University of Helsinki, for public criticism in Physicum auditorium E204, Gustaf Hällströmin katu 2a, at 12:00 noon, on April 20th, 2018.

Helsinki 2018

Author's Address: Institute for Atmospheric and Earth System Research/Physics
Faculty of Science
P.O. Box 64 (Gustaf Hällströmin katu 2a)
FI-00014 University of Helsinki
putian.zhou@helsinki.fi

Supervisors: Docent Michael Boy, Ph.D.
Institute for Atmospheric and Earth System Research/Physics
Faculty of Science
University of Helsinki

Docent Üllar Rannik, Ph.D.
Institute for Atmospheric and Earth System Research/Physics
Faculty of Science
University of Helsinki

Reviewers: Professor Hannele Hakola, Ph.D.
Atmospheric Composition Research
Finnish Meteorological Institute

Docent Harri Kokkola, Ph.D.
Atmospheric Research Centre of Eastern Finland
Finnish Meteorological Institute

Opponent: Professor Andreas Stohl, Ph.D.
Norwegian Institute for Air Research

Custos: Professor Veli-Matti Kerminen, Ph.D.
Institute for Atmospheric and Earth System Research/Physics
Faculty of Science
University of Helsinki

ISBN 978-952-7276-01-3 (printed version)
ISSN 0784-3496
Helsinki 2018
Unigrafia Oy

ISBN 978-952-7276-02-0 (pdf version)
http://ethesis.helsinki.fi
Helsinki 2018
Helsingin yliopiston verkkojulkaisut

Acknowledgements

My research in this thesis was mostly carried out at the Department of Physics in the University of Helsinki, located on a hilltop in Kumpula. I thank the previous and current heads of the Department Prof. Hannu Koskinen and Prof. Kai Nordlund for providing me a nice working environment and all the necessary working facilities. I am really grateful to the Head of the Division of Atmospheric Sciences, now the Head of the Institute for Atmospheric and Earth System Research (INAR), Prof. Markku Kulmala, for providing me the position and funding to work in a world top-level research group. I am also thankful to Maj and Tor Nessling Foundation for their funding support to my research. I thank CSC - IT Center for Science for providing me the computation resources. I am also grateful to Prof. Hannele Hakola and Dr. Harri Kokkola for their valuable comments on this thesis.

My great gratitude goes to my supervisors Dr. Michael Boy and Dr. Üllar Rannik. I worked with Michael since I was a master student, and now I am going to graduate as a doctor. We spent a lot of time together, experiencing people coming to and leaving from our modelling group. Thank you so much for the guidance and for providing me so many opportunities of teaching in different courses. I am also grateful to Üllar Rannik for the guidance and all the helpful discussions.

Here I specially thank Prof. Laurens Ganzeveld for helping me finish the modelling work which is really essential for this thesis. I am also thankful to Luxi, Ditte, Pontus, Anton, Rosa and Emilie for all the happy time and your support. I want to thank Dean, Carlton and Ben for the football discussions at lunch time. I would also like to thank all my coauthors and colleagues, without you I would not finish my work in this thesis.

I want to express my special gratitude to my Chinese community, you made me feel at home and gave me so much support. And thank you for all the parties and hikings. I also want to thank Du Mian, Zhao Kai and Liu Yanhe for all the wonderful discussion time during lunch.

Finally, I wish to thank my wife Qi Wenjuan for your unfailing support these years, and thank you for bringing me a lovely daughter who made my life totally different. I also thank my parents and parents-in-law for all your unconditional support.

A peaceful space after all the final words, to my grandma Guo Chunmei.

Putian Zhou
University of Helsinki, 2018

Abstract A large amount of biogenic volatile organic compounds (BVOCs) are emitted from boreal forests. Once emitted, BVOCs can be oxidized in the air, participate in particle formation and growth and thus indirectly affect local, regional and global climate. BVOCs act as a bridge between the biosphere and the atmosphere including atmospheric chemistry in both gas and particle phases. In this thesis we studied the in-canopy sources and sinks of BVOCs, the roles of BVOCs in gas and particle phases, as well as the impact of aerosol dynamics on the vertical aerosol fluxes in the planetary boundary layer.

Several findings in this thesis are shown below: (1) By using a newly implemented gas dry deposition model in a one-dimensional chemical transport model SOSAA (model to Simulate the concentrations of Organic vapours, Sulphuric Acid and Aerosols) we simulated the in-canopy source and sink terms of 12 featured BVOCs. According to the strength of individual terms, BVOCs were classified into five categories: Cemis in which most of the emitted gases are transported out of the canopy, Cemis-chem in which most of the emitted gases are quickly oxidized inside the canopy, Cemis-depo in which emissions are comparable to deposition, Cdepo in which the dominant deposition sink leads to downward fluxes and Cchem-depo in which the chemical production compensates a part of deposition. (2) High upward fluxes of formic acid over a boreal forest were observed. The required unknown precursors and emission sources were quantified to explain the missing sources inside the canopy. (3) The simulated O_3 concentration change due to chemical reactions related to BVOCs was in average less than 10% of the deposition sink. (4) The highly oxidized multifunctional organic molecules (HOMs) play a dominant role in the growth of new particles over the sub-Arctic forest region at the Pallas Atmosphere-Ecosystem Supersite and account for $\sim$ 75% of total SOA mass during new particle formation events. (5) The modelled vertical aerosol fluxes above the canopy caused by aerosol dynamics were comparable or sometimes exceeded that caused by particle dry deposition. This introduced large biases between measured flux and the particle dry deposition flux. The findings (1), (2), (3), (5) were obtained over the boreal forest at SMEAR (Station for Measuring Ecosystem-Atmosphere Relations) II.

This thesis provides a new numerical tool to analyse detailed sources and sinks of BVOCs, which can be applied in other ecosystems and further implemented in large-scale models.

Keywords: 1D model, dry deposition, biogenic volatile organic compounds, gas fluxes, aerosol fluxes, aerosol composition, secondary aerosol formation, new particle formation

Contents

List of publications

This thesis consists of an introductory review, followed by five research articles in the order of published or accepted time. In the introductory part, these papers are cited according to their roman numerals. **Papers I, III, IV and V** are reproduced under Creative Commons Attribution 3.0 License. **Paper II** is reproduced under the agreement between Zhou Putian (me) and John Wiley and Sons.

I Rannik, Ü., Zhou, L., **Zhou, P.**, Gierens, R., Mammarella, I., Sogachev, A., and Boy, M. (2016). Aerosol dynamics within and above forest in relation to turbulent transport and dry deposition, *Atmos. Chem. Phys.*, 16:3145–3160, https://doi.org/10.5194/acp-16-3145-2016.

II Schobesberger, S., Lopez-Hilfiker, F. D., Taipale, D., Millet, D. B., D'Ambro, E. L., Rantala, P., Mammarella, I., **Zhou, P.**, Wolfe, G. M., Lee, B. H., Boy, M., Thornton, J. A. (2016). High upward fluxes of formic acid from a boreal forest canopy, *Geophys. Res. Lett.*, 43:9342–9351, doi:10.1002/2016GL069599.

III **Zhou, P.**, Ganzeveld, L., Rannik, Ü., Zhou, L., Gierens, R., Taipale, D., Mammarella, I., and Boy, M. (2017). Simulating ozone dry deposition at a boreal forest with a multi-layer canopy deposition model, *Atmos. Chem. Phys.*, 17:1361–1379, https://doi.org/10.5194/acp-17-1361-2017.

IV Öström, E., **Putian, Z.**, Schurgers, G., Mishurov, M., Kivekäs, N., Lihavainen, H., Ehn, M., Rissanen, M. P., Kurtén, T., Boy, M., Swietlicki, E., and Roldin, P. (2017). Modeling the role of highly oxidized multifunctional organic molecules for the growth of new particles over the boreal forest region, *Atmos. Chem. Phys.*, 17:8887-8901, https://doi.org/10.5194/acp-17-8887-2017.

V **Zhou, P.**, Ganzeveld, L., Taipale, D., Rannik, Ü., Rantala, P., Rissanen, M. P., Chen, D., and Boy, M. (2017). Boreal forest BVOCs exchange: emissions versus in-canopy sinks, *Atmos. Chem. Phys.*, 17:14309-14332, https://doi.org/10.5194/acp-17-14309-2017.

1 Introduction

On the Earth, one-third of global forest regions are covered by the boreal forests which span the high latitude zones across the northern continental land over Eurasia and North America (Spracklen et al., 2008). The boreal forests are sparsely populated and therefore are not impacted much by anthropogenic activities. However, in the European boreal forests, the forest management, agricultural settlement and animal husbandry can still have a significant human impact on the tree growth, species composition and forest fires (Ruckstuhl et al., 2008). The boreal forests impact the atmospheric chemistry, the regional meteorology as well as the global climate via atmosphere-biosphere interactions.

The vegetation and soil surfaces in a boreal forest are important sinks for tropospheric O_3 (Launiainen et al., 2013; **Paper III**), which is one of the three most important oxidants in the atmosphere with the other two being the hydroxyl radical (OH) and the nitrate radical (NO_3) (Mogensen et al., 2015). In addition, troposheric O_3 impacts on the global climate by acting as an important greenhouse gas (Chap. 2, Stocker et al., 2013), damage human health as an air pollutant (Kampa and Castanas, 2008) and harm plants by affecting their functions (Felzer et al., 2007). The O_3 removal within a boreal forest, namely dry deposition in this thesis, depends on the turbulent transport within and above the canopy, the molecular diffusive motions through the quasi-laminar boundary layer near the leaf surface, the wetness conditions on the leaf surface, the plant physiology and the soil properties (Ganzeveld and Lelieveld, 1995). In **Paper III** we investigated the individual O_3 dry deposition processes within a boreal forest canopy.

The boreal forest emits a large number of biogenic volatile organic compounds (BVOCs) (Guenther et al., 2006; Rinne et al., 2009; Guenther et al., 2012). Some of them are directly emitted from various organisms inside the canopy, e.g., monoterpenes ($C_{10}H_{16}$), isoprene (C_5H_8), 2-methyl-3-buten-2-ol (MBO), sesquiterpenes ($C_{15}H_{24}$), methanol (CH_3OH), acetone ($CH_3C(O)CH_3$), formaldehyde (HCHO), acetaldehyde (CH_3CHO), etc (Rinne et al., 2009; Guenther et al., 2012). Once emitted into the atmosphere, these BVOCs will be oxidized to form other BVOCs, e.g., oxygenated volatile organic compounds (OVOCs), by reacting with oxidants in the air, mostly with OH, O_3 and NO_3 as mentioned above. Further chemical reactions can oxidize the BVOCs to carbon monoxide (CO) or carbon dioxide (CO_2) finally (Goldstein and Galbally, 2007). The

emitted and chemically-produced BVOCs are transported by the air flow and can be removed within the canopy by various dry and wet deposition pathways. A large part of gases, including BVOCs and inorganic gases, are uptaken on the leaf surface via leaf stomata and cuticle, as well as the water films formed under a high humidity condition (Wesely, 1989; Zhang et al., 2003; Niinemets et al., 2014). The dry deposition onto the soil surface also plays a significant role in a boreal forest (**Paper V**). The wet deposition, including the scavenging in convective updrafts, the washout and the rainout, is not considered important under most of the conditions studied in this thesis and is not included in the gas dry deposition model. All of these processes, including emissions, chemical reactions, turbulent transport and dry deposition, are major factors affecting BVOC fluxes over the canopy, which were investigated in **Paper II** and **Paper V**.

A part of BVOCs with low saturation vapor pressure can participate in the formation of new aerosol particles (Kulmala et al., 2013; Tröstl et al., 2016), or contribute to particle growth by condensing onto existing particles (Jimenez et al., 2009; Kulmala et al., 2013; Ehn et al., 2014). Among the OVOCs, the extremely low-volatility organic compounds (ELVOCs) were found to substantially contribute to the growth of secondary organic aerosol (SOA) (Ehn et al., 2014; Jokinen et al., 2015). In **Paper IV**, with the newly found formation pathways of highly oxidized multifunctional organic molecules (HOMs) (Ehn et al., 2014), we modelled new particle formation (NPF) events over the sub-Arctic forest region following air mass trajectories originating over the clean Artic ocean. If the condensation growth overcomes the coagulation scavenging onto pre-existing large particles, the newly formed particles can grow over 50 nm and act as cloud condensation nuclei (CCN) which are relevant to the climate (Kerminen et al., 2012). Moreover, the particles are transported throughout the planetary boundary layer (PBL) by the turbulent air flow and can be deposited inside the canopy. In **Paper I** we analysed the role of the aerosol dynamic processes (including particle formation, condensation growth, coagulation sink, deposition) in the aerosol fluxes over a boreal forest canopy.

In the boreal forests, BVOCs act as a bridge between the biosphere and the atmosphere. They are involved in the atmospheric chemistry processes in both gas and particle phases and thereby potentially impact local, regional and global climate. This thesis aims to provide new insights in the exchange of BVOCs between biosphere and atmosphere, the role of BVOCs in both gas and particle phases. The main objectives of this thesis are:

1. Quantify the sources and sinks of BVOCs within a boreal forest canopy and

explain the measured BVOC fluxes above the canopy with the model (**Papers II and V**).

2. Find out how much the chemical reactions alter O_3 concentration within a boreal forest canopy (**Paper III**).

3. Quantify the contribution of the oxidation products of BVOCs in aerosol particle formation and growth during NPF events with the model (**Paper IV**).

4. Quantify how much the aerosol dynamical processes impact the aerosol fluxes over a boreal forest canopy (**Paper I**).

2 Methods

In this thesis, the process-based modelling was the main method which was applied at different measurement sites. Meanwhile, the field observation data in individual sites along with reanalysis data were also essential to provide the input for the model simulations, to verify model performance and to constrain our analysis within a realistic and reasonable range. The measurement sites are described in details in Sec. 2.1. The modelling systems are introduced in Sec. 2.2.

2.1 Measurement sites

In **Papers I, II, III and V** the model simulations and measurements were conducted at the SMEAR (Station for Measuring Ecosystem-Atmosphere Relations) II station. The period from 1 May to 10 May in 2013 with frequent NPF events was covered in **Paper I**. In **Paper II** we analysed the results from 28 April to 3 June in 2014 during the field campaign BAECC (Biogenic Aerosols - Effects on Clouds and Climate). In **Paper III** and **Paper V** we simulated the whole month of August and July in 2010, respectively. In **Paper IV** 10 NPF events were simulated with a column model following 7-day backward trajectories ending at the Pallas Atmosphere-Ecosystem Supersite. These 10 events occurred during 2005 to 2010 (7 August 2005, 5–6 July 2006, 27–28 July 2006, 22–23 May 2007, 30–31 May 2008, 7–8 July 2008, 19–20 July 2009, 14 April 2010, 13–14 July 2010, 16 July 2010).

2.1.1 SMEAR II

The SMEAR program was first proposed at the beginning of 1990 (Hari and Kulmala, 2005) and then the SMEAR II station was established in 1995 at the Hyytiälä Forestry Field Station (Ilvesniemi et al., 2010). The SMEAR II station is located in Hyytiälä in southern Finland (61°51'N, 24°17'E, 181 m a.s.l., UTC+02) (Hari and Kulmala, 2005). Various land use types exist in the area of 1600 km^2 around the station, including $\sim$ 26% spruce dominated forest, $\sim$ 23% pine dominated forest, $\sim$ 21% mixed forest, 13% water bodies, $\sim$ 10% agriculture, as well as less than 8% areas with open land, deciduous forest, clear cut, wetlands and built areas (Haapanala et al., 2007). The station is surrounded by a rather homogeneous pine dominated forest stand nearby in

which the tree species contain 93% Scots pine (*Pinus sylvestris*), 2% Norway spruce (*Picea abies*) and deciduous trees (mainly silver birch (*Betula pendula*) and downy birch (*Betula pubescens*)), as well as 5% European aspen (*Populus tremula*) (Bäck et al., 2012). The understorey vegetation mainly consists of lingonberry (*Vaccinium vitis-idaea*) and blueberry (*Vaccinium myrtillus*) with an average height of 0.2 – 0.3 m. Mosses grow on the ground with a 5-cm humus layer underlying in the podzolic soil (Pumpanen et al., 2003; Bäck et al., 2012; Launiainen et al., 2013).

Considering the mostly homogeneous land use near the station, the canopy was assumed to be homogeneous with all the overstorey tree species as Scots pine for all the simulations in this thesis. The canopy height was $\sim$ 18 m. The all-sided leaf area index (LAI) was determined differently in individual papers. In **Papers I and II** we used all-sided LAI values of $\sim$ 6.5 m^2 m^{-2} and 6.3 m^2 m^{-2}, respectively. These two papers included the understorey vegetation in the all-sided LAI values but ignored its impacts. In **Papers III and V** we used 6.5 m^2 m^{-2} as in **Paper I**, but the deposition processes were calculated separately for overstorey ($\sim$ 6.0 m^2 m^{-2}) and understorey (0.5 m^2 m^{-2}) plants. In addition, in **Papers III and V** the understorey vegetation was considered as broad-leaved plants which was different from the overstorey needle-leaved trees. Therefore, the projected LAI was 37% and 50% of the all-sided LAI for overstorey and understorey vegetation, respectively. The moss layer was not included in this thesis.

At SMEAR II station, many meteorological, gas and aerosol measurements have been conducted routinely (Hari and Kulmala, 2005). These include, for example, wind speed, air temperature, sensible and latent heat fluxes, concentration of water vapor, CO_2, total number concentration of aerosol particles, aerosol size distributions, etc. These datasets are publicly available and can be downloaded in the AVAA data platform (https://avaa.tdata.fi/web/smart/smear; Junninen et al., 2009). Specifically, In **Paper I** we utilised the aerosol size distribution ranged from 3 nm to 1 μm at 2 m measured by a differential mobility particle sizer (DMPS) system. In **Paper II**, the concentration and flux of formic acid (HCOOH) was measured by a high-frequency (10 Hz) sonic anemometer (METEK USA-1) and an Iodide-Adduct High-Resolution Time-of-Flight Chemical Ionization Mass Spectrometer (CIMS) at 35 m (Lee et al., 2014). The routinely measured O_3 concentrations and fluxes were used in **Paper III**. The BVOC fluxes used in **Paper V** were computed with the surface-layer-profile method (Rannik, 1998; Rantala et al., 2014), which employed the BVOC concentra-

tions measured by a proton transfer reaction quadrupole mass spectrometer (PTR-MS, manufactured by Ionicon Analytik GmbH, Innsbruck, Austria).

2.1.2 Pallas

The Pallas Atmosphere-Ecosystem Supersite (67.97°N, 24.12°E, 565 m a.s.l.) is located about 170 km north of the Arctic Circle in Muonio, Lapland. The station is about 100 m above the tree line and surrounded mainly by low vascular plants, mosses and lichen (Lohila et al., 2015). The area around the station is very sparsely populated with the nearest city Muonio 20 km away in the south-west direction (Kivekäs et al., 2009). Therefore, there are very few local or regional air pollutants impacting on the measurement site, which makes it an excellent place to provide the observation of background air composition (Lohila et al., 2015).

Most of the instruments in the site are operated by Finnish Meteorological Institute (FMI), measuring, e.g., concentrations of CO_2, O_3 and VOC, total number concentration and size distributions of aerosol particles, aerosol optical properties, etc. Among these measurement data, the particle size distribution measured by a DMPS in the range of 7 to 500 nm (Kivekäs et al., 2009) and the particle chemical composition measured by an aerosol mass spectrometer (AMS) (Jaatinen et al., 2014) were used in **Paper IV**.

2.2 Applied modelling systems

The 1D chemical transport model SOSAA (model to Simulate the concentrations of Organic vapours, Sulphuric Acid and Aerosols) is applied in **Papers I, II, III and V** and is thus the main numerical tool in this thesis. In **Paper IV** we used the 1D version of the trajectory model ADCHEM (Aerosol Dynamics, gas and particle phase CHEMistry and radiative transfer model) in order to simulate the chemistry and aerosol processes along the air mass trajectories.

2.2.1 SOSAA

2.2.1.1 Introduction

SOSAA was originally developed by Boy et al. (2011) which was a one-dimensional (1D) chemical transport model named as SOSA (a new model to Simulate the concentrations of Organic vapours and Sulphuric Acid). Since then, it was applied in several subsequent studies (e.g., Kurtén et al., 2011; Mogensen et al., 2011; Bäck et al., 2012; Boy et al., 2013; Smolander et al., 2014). In 2014, Zhou et al. (2014) added a new aerosol module into SOSA to compute detailed aerosol processes, which renamed SOSA to SOSAA. After that, a new gas dry deposition module was implemented to close the sources and sinks of gas species in the model (**Papers III and V**). Therefore, the current SOSAA contains five coupled modules and is able to simulate BVOC emissions, chemical reactions in the air, aerosol dynamics as well as the vertical transport of gas species and aerosol particles in the PBL. A simplified diagram of SOSAA is shown in Fig. 1.

The meteorology part of SOSAA is based on the 1D version of SCADIS (SCAlar DIStribution) which is a three-dimensional (3D) RANS (Reynolds-averaged Navier-Stokes)-based turbulence model (Sogachev et al., 2002). The prognostic meteorological quantities are computed every time step, including west and south wind velocities (u and v), air temperature (T), absolute humidity (ρ_v), turbulent kinetic energy (TKE) and the specific rate of TKE dissipation (ω). The ERA-Interim reanalysis data provided by the European Centre for Medium-Range Weather Forecasts (ECMWF, Dee et al., 2011) are used to constrain the upper boundary conditions of u, v, T and ρ_v, representing a synoptic-scale meteorological impact on the model domain. In the lower levels near or inside the canopy, the values of these four variables are nudged toward local observations. Several other parameters can also be read in if possible to improve the energy balance closure, e.g., the measured incoming direct and diffuse global radiations at the canopy top, the measured soil heat flux, the long wave radiation from the sky obtained from the ERA-Interim dataset, etc.

A modified version of MEGAN 2.04 (Model of Emissions of Gases and Aerosols from Nature; Guenther et al., 2006) described in Mogensen et al. (2015) is implemented to compute the BVOC emissions from different ecosystems. In this thesis only the boreal pine-dominated forest is considered (**Paper V**). Currently, the emissions of

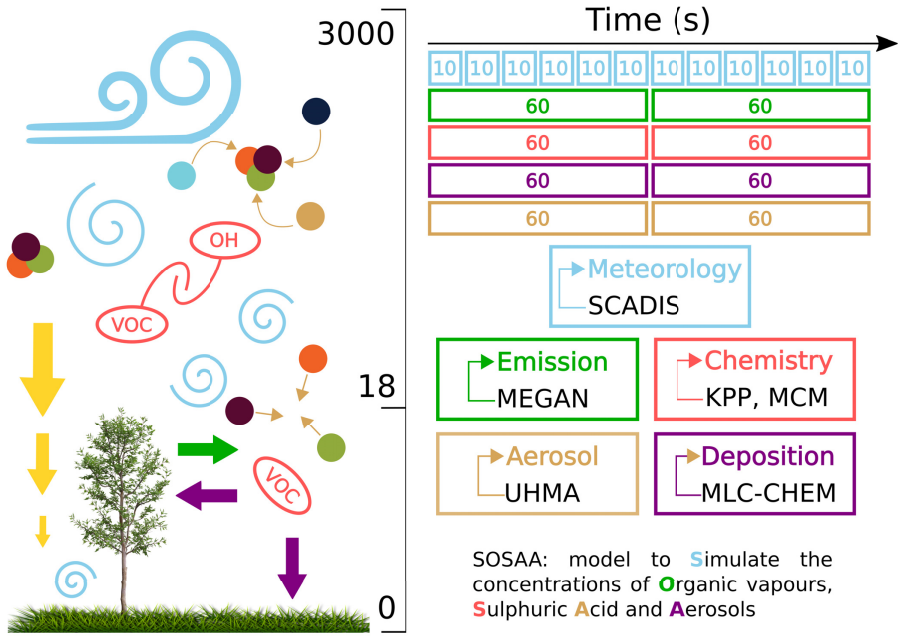

Figure 1: A simplified diagram of SOSAA. Different modules are marked by different colors, blue for meteorology, green for emission, red for chemistry, brown for aerosol and purple for deposition. The meteorology module is computed every 10 s, other modules are computed every 60 s. The three downward yellow arrows on the lower left corner represent radiation attenuation inside the canopy.

15 BVOCs or groups of BVOCs are calculated in the emission module, including α-pinene, β-pinene, Δ^3-carene, limonene, 1,8-cineole, other minor monoterpenes (OMT), β-caryophyllene, farnesene, other minor sesquiterpenes (OSQ), isoprene, 2-methyl-3-buten-2-ol (MBO), methanol, acetaldehyde, acetone and formaldehyde.

The chemistry module is generated by KPP (Kinetic PreProcessor; Damian et al., 2002) with the the chemical scheme obtained from MCMv3.3.1 (Master Chemical Mechanism version 3.3.1; http://mcm.leeds.ac.uk/MCM) (Jenkin et al., 1997; Saunders et al., 2003; Jenkin et al., 2012). A commonly-used chemistry scheme for a boreal forest will include (1) necessary inorganic reactions, (2) the full oxidation paths of α-pinene, β-pinene,

limonene, β-caryophyllene, isoprene, MBO and methane (CH_4), (3) the first-order oxidation reactions with OH, O_3 and NO_3 for other emitted gas compounds, e.g., Δ^3-carene, 1,8-cineole, OMT, farnesene, OSQ, etc. (Atkinson, 1997), (4) Other specific reactions, e.g., the reactions related to stabilized Criegee intermediates (sCIs) (Boy et al., 2013). The concentrations of nitric oxide (NO), nitric dioxide (NO_2), sulfur dioxide (SO_2), carbon monoxide (CO), CH_4, hydrogen (H_2) are obtained from the measurement data. The condensation sinks of sulfuric acid (H_2SO_4) and nitric acid (HNO_3) are computed according to Pirjola et al. (1999) and Kulmala et al. (2001), serving as an input for the model runs.

The aerosol microphysics is computed by UHMA (University of Helsinki Multicomponent Aerosol model; Korhonen et al., 2004), including nucleation, condensation growth, coagulation sinks and deposition (Zhou et al., 2014). The particle number size distribution is initialized with the measured data at 2 m height every midnight in order to constrain it in a realistic range.

The gas dry deposition module is derived from the Multi-Layer Canopy CHemistry Exchange Model (MLC-CHEM; Ganzeveld et al., 2002) which was first developed by Ganzeveld and Lelieveld (1995) and Ganzeveld et al. (1998). In **Paper I** we did not include a gas dry deposition module. However, although the currently-used extended gas dry deposition module was publicly implemented in **Paper V**, it was already used in **Papers II and III**. More details of the deposition module are shown in Sec. 2.2.1.2.

The model domain in SOSAA is usually set from 0 m at the surface up to 3 km with 51 logarithmically-distributed layers, including the whole PBL and the lower part of free atmosphere. The time integration method is semi-implicit, and the time step of the meteorology is set to 10 s. The other four modules are computed every 60 s, which saves the computation time. SOSAA is programmed in Fortran90 and is designed to be able to run in parallel in supercomputers.

2.2.1.2 Gas dry deposition module

In this thesis, we only consider the dry deposition onto leaf and soil surfaces, and neglect the deposition onto other surfaces, e.g., trunks, branches, bare roots, etc. Hence, the local concentration change of the gas compound X (ng m^{-3}) with time t (s) can be

calculated as

$$\frac{\partial[X]}{\partial t} = Q_{emis} + Q_{chem} + Q_{turb} - [X](\mathrm{LAD} \cdot V_{dveg} + A_s V_{dsoil}), \tag{1}$$

where Q_{emis} is the emission source, Q_{chem} is the net chemical production and loss, and Q_{turb} represents the concentration change due to turbulent transport. LAD ($m^2\ m^{-3}$) is the all-sided leaf area density, which is obtained from the all-sided LAI and the vertical distribution of vegetation density. A_s ($m^2\ m^{-3}$) is the soil area index. V_{dveg} ($m\ s^{-1}$) is the layer-specific conductance of vegetation and V_{dsoil} ($m\ s^{-1}$) is the soil conductance. They can be calculated with a resistance analogy parameterization method as shown in Fig. 2.

For vegetation part,

$$V_{dveg} = \frac{1}{r_{veg}} \tag{2}$$

Here r_{veg} ($s\ m^{-1}$) is the total leaf surface resistance which is calculated differently for needle and broad leaves. For needle leaves, the stomata exist on all the sides, so r_{veg} can be calculated as

$$r_{veg} = r_b + \frac{1}{1/(r_{stm} + r_{mes}) + (1 - f_{wet})/r_{cut} + f_{wet}/r_{ws}}. \tag{3}$$

Here r_b ($s\ m^{-1}$) is the quasi-laminar boundary layer resistance above the leaf surface. It is determined by the molecular diffusivity and horizontal wind speed (Meyers, 1987),

$$r_b = \frac{\mathrm{Sc}^{2/3}}{0.66\nu^{1/2}}\sqrt{\frac{l_d}{U}} \tag{4}$$

$$\mathrm{Sc} = \frac{\nu}{D_X} \tag{5}$$

$$D_X = D_{\mathrm{H2O}}\sqrt{\frac{M_{\mathrm{H2O}}}{M_X}} \tag{6}$$

Here Sc (dimensionless) is the Schmidt number of gas X which is the ratio of kinematic viscosity for air ($\nu = 1.59 \times 10^{-5}\ m^2\ s^{-1}$) and molecular diffusivity (D_X; $m^2\ s^{-1}$). D_X is estimated according to Graham's law in which D_{H2O} is $2.4 \times 10^{-5}\ m^2\ s^{-1}$ and M ($g\ mol^{-1}$) is the molar mass. l_d (0.07 m) is the leaf length scale along the mean wind direction. U ($m\ s^{-1}$) is the horizontal wind speed above the leaf surface. r_{stm} ($s\ m^{-1}$) is the stomatal resistance which can be converted from the stomatal resistance of water vapour ($r_{stm,\mathrm{H_2O}}$; $s\ m^{-1}$),

$$r_{stm} = \frac{D_{\mathrm{H_2O}}}{D_X} r_{stm,\mathrm{H_2O}} \tag{7}$$

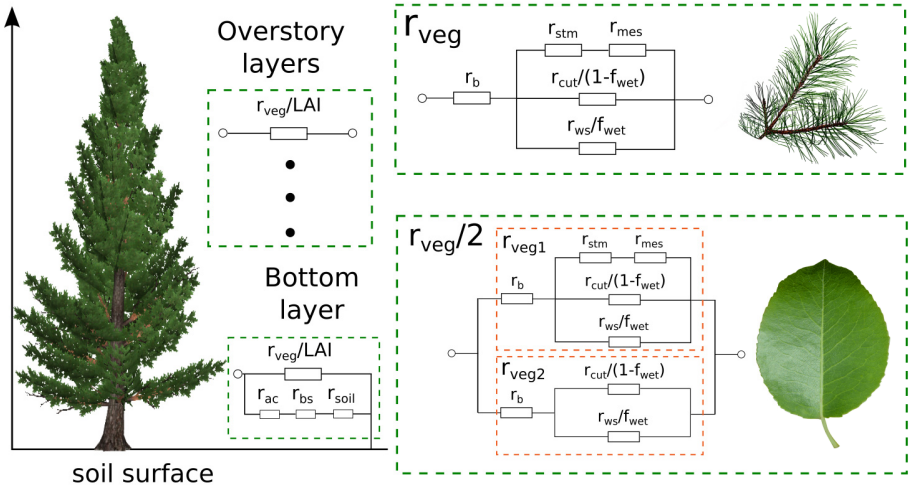

Figure 2: The diagram of resistance analogy method used in the gas dry deposition model. The overstorey layers and the bottom layer are considered separately. The bottom layer includes the broad-leaved understorey vegetation and soil surface. r_{ac} is the resistance representing the turbulent transport from the reference height of the understorey vegetation to the soil surface. r_{bs} is the soil boundary layer resistance. r_{soil} is the soil resistance. r_b is the quasi-laminar boundary layer resistance above the leaf surface. r_{veg} represents the resistance to vegetation leaves, which is plotted on the right-hand side in details. For broad leaves, the resistance to the side with (r_{veg1}) or without (r_{veg2}) stomata is computed separately. r_{stm} is the stomatal resistance and r_{mes} is the mesophyllic resistance. r_{cut} is the cuticular resistance and r_{ws} is the resistance to wet skin. f_{wet} is the wet skin fraction. All the variables are defined for each model layer. Note that here LAI is the all-sided leaf area index for each layer. The symbols are also explained in the text.

$r_{stm,\mathrm{H_2O}}$ can be computed in the meteorology module. r_{mes} (s m^{-1}) is the mesophyllic resistance which can be set to 0 for O_3 and SO_2. r_{cut} (s m^{-1}) is the cuticular resistance which is 10^5 s m^{-1} for O_3 and SO_2. r_{ws} (s m^{-1}) represents the leaf wet skin uptake which is 2000 s m^{-1} for O_3 and 100 s m^{-1} for SO_2. f_{wet} is the wetness fraction on the leaf which is dependent on the relative humidity (RH; dimensionless) (Lammel, 1999; Wu et al., 2003). At SMEAR II, the water films start to form when RH is over about

0.7 (or 70%) (Altimir et al., 2006), hence f_{wet} is calculated as

$$f_{wet} = \begin{cases} 1 & 0.9 \leqslant \mathrm{RH} \\ \frac{\mathrm{RH}-0.7}{0.2} & 0.7 \leqslant \mathrm{RH} < 0.9 \\ 0 & \mathrm{RH} < 0.7 \end{cases} . \tag{8}$$

For broad leaves, stomata usually only exist in one side which is facing down. Therefore, the leaf surface resistance should be calculated for two sides separately,

$$r_{veg} = 2 \Big/ \left(\frac{1}{r_{veg1}} + \frac{1}{r_{veg2}} \right) \tag{9}$$

$$r_{veg1} = r_b + \frac{1}{(1 - f_{wet})/r_{cut} + f_{wet}/r_{ws}} \tag{10}$$

$$r_{veg2} = r_b + \frac{1}{1/(r_{stm} + r_{mes}) + (1 - f_{wet})/r_{cut} + f_{wet}/r_{ws}}. \tag{11}$$

Here the factor 2 in Eq. 9 is added because each side only counts for half of the all-sided LAD. r_{veg1} (s m^{-1}) and r_{veg2} (s m^{-1}) represent the leaf surface resistances to the sides without and with stomata, respectively.

The deposition onto the soil surface is further calculated as,

$$V_{dsoil} = \frac{1}{r_{ac} + r_{bs} + r_{soil}}, \tag{12}$$

where r_{ac} (s m^{-1}) represents the difficulty of transfering a gas molecule to pass through the canopy to the soil surface. In this thesis, r_{ac} is ignored because the turbulent transport inside the canopy is explicitly calculated in SOSAA. The soil boundary layer resistance r_{bs} can be obtained as (Nemitz et al., 2000; Launiainen et al., 2013),

$$r_{bs} = \frac{\mathrm{Sc} - \ln(\delta_0/z_*)}{\kappa u_{*g}}. \tag{13}$$

δ_0 is the height where the molecular diffusivity is the same as the turbulent eddy diffusivity and is calculated as,

$$\delta_0 = \frac{D_X}{\kappa u_{*g}} \tag{14}$$

κ (dimensionless) is the von Kármán constant (0.41) and u_{*g} (m s^{-1}) is the friction velocity on the ground surface. z_* is the height below which the logarithmic wind profile is assumed. r_{soil} (s m^{-1}) is the soil resistance, 400 s m^{-1} for O_3 and 250 s m^{-1} for SO_2.

For other compounds than O_3 and SO_2, several resistances need to be revised according to the chemical properties of individual gas species. In this thesis, a parameterization method modified from Wesely (1989) and Nguyen et al. (2015) is used,

$$r_{stm} = \frac{D_{\mathrm{H2O}}}{D_X} r_{stm,\mathrm{H2O}} \tag{15}$$

$$r_{mes} = \left(\frac{H}{50RT_l} + 100 f_0 \right)^{-1} \tag{16}$$

$$r_{cut} = \left(\frac{10^{-4}H}{RT_l} + f_0 \right)^{-1} r_{cut,\mathrm{O3}} \tag{17}$$

$$r_{ws} = \left(\frac{1}{3r_{ws,\mathrm{SO2}}} + \frac{10^{-6}H}{RT_l} + \frac{f_0}{r_{ws,\mathrm{O3}}} \right)^{-1} \tag{18}$$

$$r_{soil} = \left(\frac{10^{-4}H}{RT_l r_{soil,\mathrm{SO2}}} + \frac{f_0}{r_{soil,\mathrm{O3}}} \right)^{-1} \tag{19}$$

Here H (M atm^{-1}) is the Henry's law constant which describes the water solubility of a compound. The larger H is, the more water soluble it is. f_0 (dimensionless) is the reactivity factor taken from three values 0, 0.1 and 1, representing non-reactive, slightly-reactive and reactive gases, respectively. R (0.082 atm M^{-1} K^{-1}) is the gas constant and T_l (K) is leaf temperature.

2.2.1.3 Henry's law constants and reactivity factors

The Henry's law constant of a specific gas compound is obtained in a priority order. First, we try to use the most reliable value in the dataset provided by Sander (2015). If the compound is not in the dataset list, the group method of model HENRYWIN (Hine and Mookerjee, 1975; Meylan and Howard, 1991) in the software EPI Suite v4.11 (US EPA, 2017) will be applied to calculate the H value. If this is not possible, the bond method of HENRYWIN will be used instead. Finally, the H values of HNO_3 and hydrogen peroxide (H_2O_2) are manually set to 10^{14} M atm^{-1} and 5×10^7 M atm^{-1} according to Nguyen et al. (2015). For all the other compounds whose H values can not be obtained with the above-mentioned methods, their H values are set to 0, implying that they can not deposit via dissolving in water.

The reactivity factors are determined according to the values provided by and the rules suggested by Wesely (1989), Karl et al. (2010), Knote et al. (2015) and Ashworth et al. (2015). More details refer to **Paper V**.

2.2.2 ADCHEM

ADCHEM is a two-dimensional (2D) Lagrangian model with turbulent diffusion calculated in horizontal and vertical directions perpendicular to the air mass trajectory (Roldin et al., 2011). In addition, ADCHEM includes detailed aerosol dynamics, gas-phase and particle-phase chemistry, in-cloud aerosol processing and a radiative transfer model. Therefore, ADCHEM is suitable for studies of regional NPF events.

In this thesis, ADCHEM is used as a 1D model with only vertical dispersions of scalars (**Paper IV**). The air mass trajectories are calculated with the Hybrid Single Particle Lagrangian Integrated Trajectory Model (HYSPLIT) (Stein et al., 2015) and downloaded from the NOAA (National Oceanic and Atmospheric Administration) Air Resource Laboratory Real-time Environmental Application and Display sYstem (READY) (Rolph et al., 2017). The meteorology data used to drive HYSPLIT are from the Global Data Assimilation System (GDAS). Other input data for ADCHEM are all retrieved along the air mass trajectories.

The land use data are obtained from the Global Land Cover Map for the Year 2000, GLC2000 database, European Commission Joint Research Centre (http://forobs.jrc.ec.europa.eu/products/glc2000/products.php). The anthropogenic gas emissions are retrieved from the EMEP (European Monitoring and Evaluation Programme) database (EMEP/CEIP 2014, http://www.ceip.at/webdab_emepdatabase/emissions_emepmodels/). The biogenic emissions are calculated with LPJ-GUESS (Lund-Potsdam-Jena General Ecosystem Simulator) (Smith et al., 2014). The wind-generated marine aerosol emissions are estimated with a parameterization method suggested in Mårtensson et al. (2003). And the primary particle emissions from ship and road traffic are converted from SO_2 (Beecken et al., 2015) and NO_x emissions (Kristensson et al., 2004), respectively. In Paper IV, either the kinetic nucleation or an organic nucleation parameterization method (Roldin et al., 2015) was used. In the latter method, a first-generation oxidation product formed from monoterpenes reacting with OH is assumed to participate in the particle formation together with sulfuric acid. Besides H_2SO_4, HNO_3, NH_3, HCl, around 700 organic species can condense onto the particles and alter their chemical composition. 63 of the condensable organic compounds represent monoterpene peroxy radical autoxidation products of which a majority are HOMs.

3 Results and discussions

3.1 BVOC fluxes above the canopy

BVOCs can be emitted from inside the canopy or produced via chemistry in the air. If we consider the canopy as a container, then BVOC fluxes at the canopy top are just the quantities representing the exchange between the canopy and the upper air. In **Papers III and V**, we developed and validated a new multi-layer gas dry deposition model in SOSAA. This enabled us to simulate the BVOC fluxes above the forest canopy in a more realistic way, especially for those compounds observed to show bi-directional fluxes.

In **Paper V**, the modelled monthly-averaged diurnal patterns of six emitted BVOCs or groups of BVOCs (monoterpenes, isoprene+MBO, methanol, acetaldehyde, acetone, formaldehyde) were compared with the observation in June 2007 at SMEAR II, which showed a good agreement considering the day-to-day variation and measurement uncertainties (Fig. 3). The diurnal cycles of monoterpenes, isoprene+MBO, methanol, acetaldehyde and acetone mostly follow the daily variations of air temperature and incoming photosynthetically active radiation (PAR), implying that the emissions dominate the fluxes. However, at nighttime and in the early morning, the deposition dominates over other processes for methanol and acetaldehyde, resulting in downward fluxes in both model and measurement. This may be due to the effective deposition onto the water films on the leaf, which was also observed in a Mediterranean oak-hornbeam forest (Schallhart et al., 2016). The measured diurnal flux of formaldehyde does not show apparent pattern, which could partly result from the large measurement uncertainties due to the low proton affinity of formaldehyde (Rantala et al., 2015).

In **Paper II**, the flux of formic acid was measured over a boreal forest canopy at SMEAR II from 28 April to 3 June 2014. We found that the net flux of formic acid was mostly upward with an average midday exchange velocity V_{ex} of 0.7 ± 1.7 cm s^{-1}. This result contradicts somehow with other observations, e.g. Kuhn et al. (2002) showed a negative V_{ex} of -0.2 cm s^{-1} during wet season over Amazon, and Nguyen et al. (2015) observed an average midday V_{ex} of -1 ± 0.4 cm s above a forest in southeastern U.S. Moveover, the high upward values were always associated with high temperature and incoming global radiation, and the downward flux usually occurred under high RH.

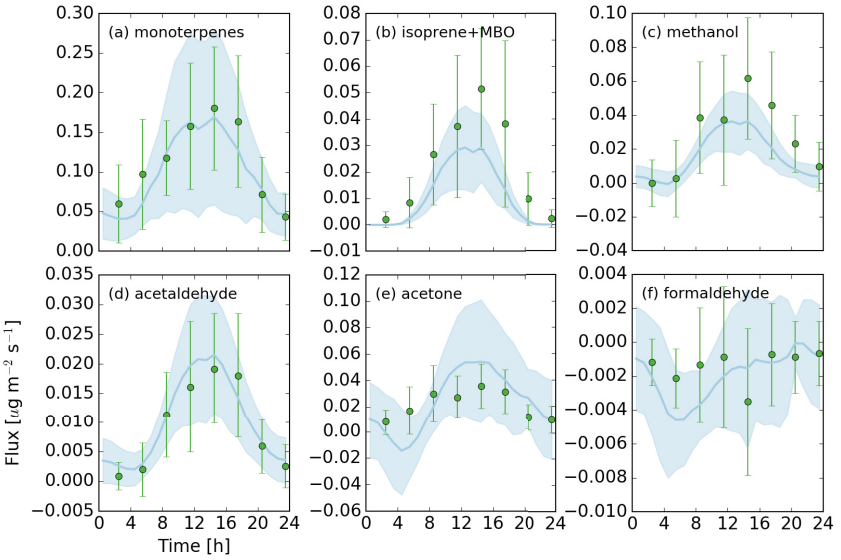

Figure 3: Modelled (blue lines) and measured (green points) monthly-averaged diurnal cycles of fluxes for (a) monoterpenes, (b) isoprene+MBO, (c) methanol, (d) acetaldehyde, (e) acetone and (f) formaldehyde at the canopy top. The ranges of ±1 standard deviation for modelled and measured data are marked by shaded areas and vertical lines, respectively. The x labels and y labels of the left bottom subfigure also apply to all the other subfigures. This figure is replotted from Fig. 4 in **Paper V**.

3.2 In-canopy sources and sinks of BVOCs

The BVOC fluxes over the canopy are mostly determined by the net production and loss of BVOCs inside the canopy. Therefore, the in-canopy sources and sinks are analysed to reveal the driving factors of BVOC fluxes. The source and sink terms include gas emissions, chemical production and loss, turbulent transport and dry deposition. Here source is a term which causes positive local concentration tendency of a compound while sink reduces the local concentration. It should be noted that the downward turbulent transport above the canopy is a source term for the canopy container, which is defined in a different way as in a micro-meteorology context.

In **Paper V** we analysed 12 featured BVOCs or groups of BVOCs, including monoterpenes, isoprene, MBO, sesquiterpenes, acetaldehyde, methanol, acetone, formaldehyde, acetol, pinic acid, BCSOZOH (one of β-caryophyllene's oxidation products), ISOP34OOH and ISOP34NO3 (both are isoprene's oxidation products). Figure 4 shows the modelled monthly-averaged relative contributions of integrated in-canopy source and sink terms. During the whole day, most of the emitted monoterpenes ($\sim$ 86%) and isoprene+MBO ($\sim$ 93%) are transported out of the canopy. At nighttime, the sink terms chemical removal and dry deposition dominate inside the canopy for isoprene+MBO, when the emission is limited and the stratification is stable near the ground. For the extremely reactive compounds sesquiterpenes, $\sim$ 71% of the emitted quantity is oxidized inside the canopy with the rest transported out. For the other emitted gases studied here, including acetaldehyde, methanol, acetone and formaldehyde, dry deposition can balance out a part or all of the emissions, resulting in possible bi-directional fluxes above the canopy. For non-emitted gases acetol, pinic acid and BCSOZOH, dry deposition is the only dominant sink term, resulting in downward fluxes. ISOP34OOH and ISOP34NO3 show similar patterns at nighttime, while at daytime the dry deposition sink can be partly or largely compensated by the chemical production. The chemical production can even exceed the deposition at noon for ISOP34NO3.

The in-canopy sources and sinks of formic acid integrated from 0 m to the flux measurement height at 39 m were analysed in **Paper II**. The direct emission from vegetation and soil is the largest source term, about one order of magnitude larger than the chemical production to our current knowledge (Fig. 5). Dry deposition is the dominant sink and chemical loss can be neglected. However, we found that the calculated source terms (emission and chemical production) were about one order of magnitude smaller than the sink terms (measured upward fluxes and calculated dry deposition) with current emission potentials and chemical yields of formic acid. Hence, this could not explain the prevalent upward fluxes during the measurement period, which thus indicated that a large portion of missing sources, e.g., emission sources or new chemical pathways, still exist.

According to relative contributions of individual source and sink terms, the BVOCs analysed above can be classified into five categories: Cemis (monoterpenes, isoprene+MBO) in which most of the emitted gases are transported out of the canopy, Cemis-chem (sesquiterpenes) in which most of the emitted gases are quickly oxidized

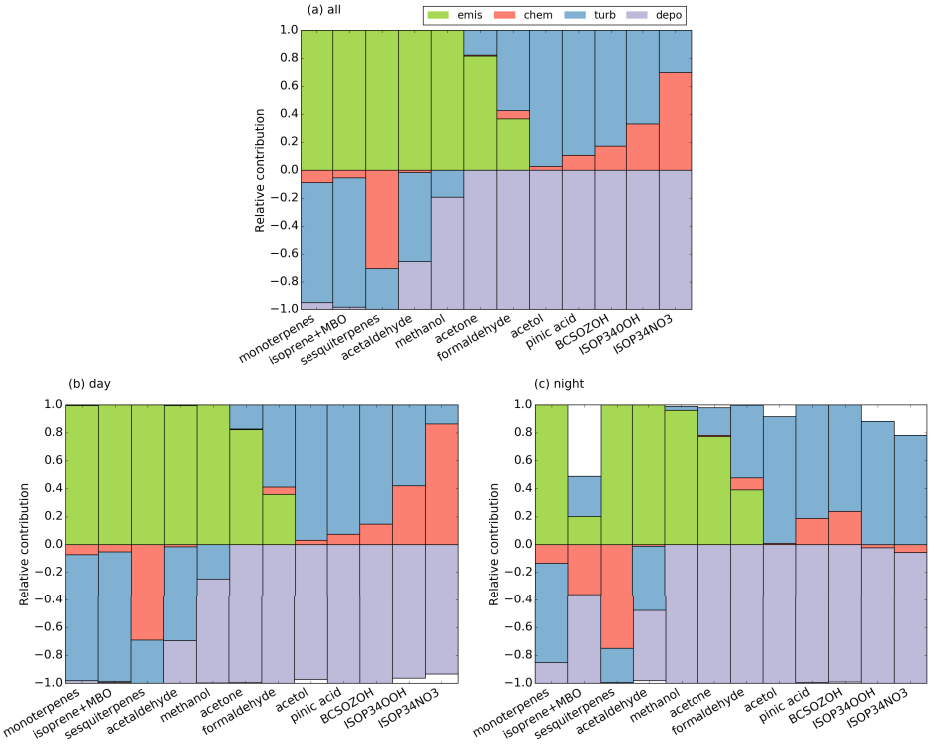

Figure 4: Monthly-averaged relative contributions of in-canopy sources and sinks, including gas emissions (emis, green), net chemical production and loss (chem, red), turbulent transport (turb, blue) and gas dry deposition (depo, purple) for selected BVOCs during (a) the whole month (all), (b) daytime (day) and (c) nighttime (night). This figure is replotted from Fig. 5 in **Paper V**.

inside the canopy, Cemis-depo (acetaldehyde, methanol, acetone, formaldehyde, formic acid) in which emissions are comparable to deposition, Cdepo (acetol, pinic acid, BCSOZOH) in which the dominant deposition sink leads to downward fluxes and Cchem-depo (ISOP34OOH, ISOP34NO3) in which the chemical production compensates a part of deposition.

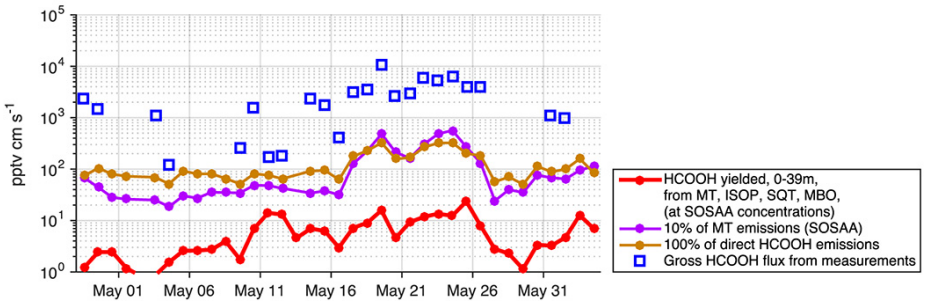

Figure 5: Midday mean HCOOH fluxes obtained by integrating production rates from ground up to 39 m (red), 10% of the total monoterpene emission flux (purple), direct HCOOH emission flux (brown), and the measured fluxes plus calculated deposition flux (bluesquares; using only midday data and the highest quality flux periods; pptv cm s−1). This figure is from Fig. 3 in **Paper II**.

In general, this classification method is most probably valid for various BVOCs also in other ecosystems at least in summer as we discussed in **Paper V**. This enables us to qualitatively analyse the characteristics of a classified BVOC. Moreover, the deposition model can be applied in large-scale models in future and thus quantify the global sources and sinks of BVOCs.

3.3 Influence of BVOCs

BVOCs in the air can directly alter the atmosphere chemistry and indirectly impact on global climate, air quality and human health through aerosol precursors. In this thesis we will focus on two specific aspects of their influence, one is how much the BVOCs can contribute to O_3 production and loss compared to other processes at SMEAR II (Sec. 3.3.1) and the other is the role of BVOCs in particle growth at Pallas (Sec. 3.3.2).

3.3.1 Role of BVOCs in O_3 removal

Dry deposition is a dominant sink term of O_3 inside the canopy (**Paper III**). However, due to complicated known and yet unknown chemical reactions related to O_3, the contribution of air chemistry to in-canopy O_3 removal is still debatable and may vary

with locations and time. BVOCs may play a significant role in the O_3 concentration change because they can either destroy or produce O_3. For example, Wolfe et al. (2011) found that additional unidentified very reactive BVOCs were necessary to explain the non-stomatal O_3 uptake in a Poderosa pine forest in the U.S. However, the air chemistry was not considered to contribute much to O_3 concentration tendency at SMEAR II (Rannik et al., 2012). Previous studies at SMEAR II only used simpified chemistry scheme to investigate the contribution of chemical removal of O_3 (Rannik et al., 2012; Launiainen et al., 2013). In this thesis, we applied SOSAA with a detailed chemistry scheme as described in Sec. 2.2.1.1 to provide a more accurate estimation.

Figure 6 shows the period-averaged (from 5 to 14 August, 2010) diurnal variations of O_3 fluxes caused by deposition (F_{depo}) and chemistry (F_{chem}), as well as the ratio between them. Here the chemistry is the net chemical production and loss of O_3 within the canopy. The air chemistry acts as a source for O_3 from $\sim$ 06:00LT (local time) to $\sim$ 15:00LT and as a sink at other time. Most values of F_{chem} lie in the range of -0.02 to 0.03 μg m^{-2} s$-$1, about one order of magnitude smaller than F_{depo} which is in the range of about 0 to -0.6 μg m^{-2} s$-$1 (Fig. 6a). The relative contribution of air chemistry also varies with time. At nighttime, the largest contribution is about 9% of deposition sink. And at daytime, up to 4% of deposition is balanced out by air chemistry. However, at some specific time points, usually at night or in the early morning, the ratio between F_{chem} and F_{depo} can reach about 24% and -20%. Therefore, air chemistry generally plays a minor role in altering in-canopy O_3 concentration, but during some specific time periods the impact can not be ignored.

3.3.2 Role of HOMs in particle growth

Recently the existence of HOMs, whose O:C ratio is greater than or equal to 0.7, have been reported in both lab and field studies (Ehn et al., 2014; Jokinen et al., 2015). Many of them have low volatility, e.g., the saturation mass concentration (C^*) of ELVOCs (extremely low volatility organic compounds) is smaller than $10^{-4.5}$ μg m^3 (the corresponding saturation molecular concentration N^* is smaller than 5×10^4 cm^{-3} if we assume the molar mass is 300 g mol^{-1}), and for LVOCs (low volatility organic compounds) C^* is in the range of $10^{-4.5}$ to $10^{-0.5}$ μg m^3 ($5 \times 10^4 \leqslant N^* \leqslant 5 \times 10^8$cm^{-3}). Other HOMs are SVOCs (semi-volatile organic compounds) which have higher volatility ($10^{-0.5}$ μg m^3 $\leqslant C^* \leqslant 10^{2.5}$ μg m^3; $5 \times 10^8 \leqslant N^* \leqslant 5 \times 10^{11}$cm^{-3}) (Tröstl et al.,

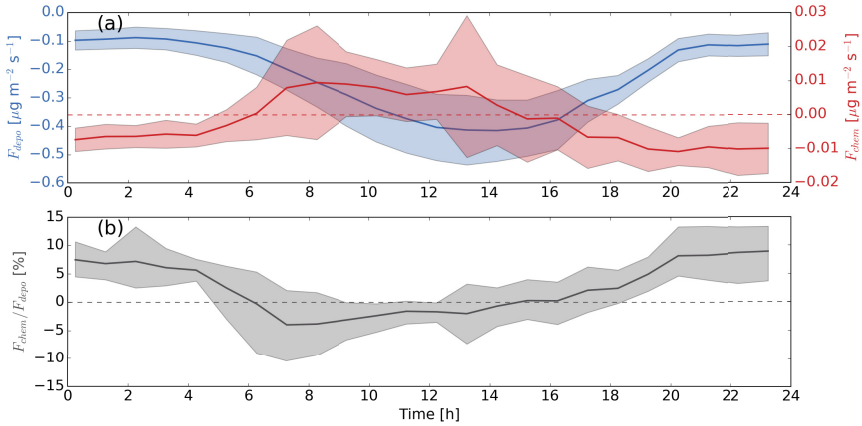

Figure 6: (a) The daily averaged (from 5 to 14 August) production and loss caused by chemistry (F_{chem}, red) and dry deposition (F_{depo}, blue). (b) The ratio between F_{chem} and F_{depo}. Zero lines for F_{chem} and the ratio are plotted as dashed lines. Shaded areas show the range of ± 1 SD. This figure is from Fig. 10 in **Paper III**.

2016). HOMs can participate in particle growth and some ELVOCs are even considered to be able to participate in NPF as described in Sec. 2.2.2.

In **Paper IV** we modelled 10 NPF events at Pallas with an updated version of ADCHEM considering the newly found HOMs generation mechanisms and their molar yields from precursor gases (Ehn et al., 2014; Jokinen et al., 2015), In total we performed simulations along 136 air mass trajectories starting 7 days backward in time along air mass trajectories mainly originating over the Arctic Ocean. The model results were evaluated by comparing the measured and modeled median number concentrations of particles larger than 7 nm (N_7) and 50 nm (N_{50}) in diameter (Fig. 7). The model overestimated N_7 at the beginning of NPF cases, which could result from a generally too early onset of the NPF event or a too high growth rates between 1.5 and 7 nm in diameter. The temporal variation pattern of N_{50} was predicted well by the model, but the maximum value occurring around 6 am the day after the NPF event were underestimated with 33% (1109 cm^{-3} compared with 1674 cm^{-3}). This may be due to the underestimated SVOC formation rates or lack of heterogeneous reactions, which can facilitate the growth of Aitken and accumulation mode particles. However,

considering both the model and measurement uncertainties the agreement between the model and observations strongly support that the formation and growth of new particles is generally captured well by the model. Without HOMs the newly formed particles rarely grow above 7 nm in diameter (Fig. 7a) and the contribution of the NPF events to N_{50} the day after the event become negligible (Fig. 7b). This demonstrates the crucial role of HOMs for the growth of new particles into the cloud condensation size range.

In average, the HOMs contributed to 75% of the modeled PM1 SOA mass, implying the dominant role of HOMs in particle growth. Compared to the reported O:C ratio of 0.73 (Ng et al., 2010), the modeled O:C in the SOA is substantially larger (0.99). However, considering the recent revision of how to calculate the elemental composition from HR-ToF-AMS data Canagaratna et al. (2015), the O:C ratio from Ng et al. (2010) should be increased with 27% and then reach a value of 0.93 which is in close agreement with the modelled O:C ratio.

3.4 Aerosol fluxes within and above the canopy

As discussed in Sec. 3.3.2, HOMs play a dominant role in the particle growth and thus participate in aerosol dynamics. The timescale of aerosol dynamics varies with particle size and individual processes. A typical range of it is between 10^3 and 10^5 s (Pryor and Binkowski, 2004), which is estimated to be in the same order of magnitude as the timescale for aerosol dry deposition (Pryor and Binkowski, 2004). Therefore, the aerosol fluxes above the canopy are determined not only by dry deposition, but also by aerosol dynamics. This will introduce systematic biases when calculating particle deposition velocities from measured fluxes. In **Paper I**, in order to quantify the impact of aerosol dynamics on particle exchange above the canopy, we analysed the magnitudes of particle turbulent transfer, dry deposition and aerosol dynamics at SMEAR II.

The NPF events during 10 consecutive days from 1 May to 10 May 2013 were simulated with SOSAA. The measured aerosol size distribution at 2 m were read in every midnight at 00:00LT as the initial value from the surface to a prescribed height (H_P). Above the H_P the aerosol concentration is set to 10% of that below the H_P. The H_P was defined as the highest PBL height in previous day. A typical nighttime stable boundary layer (SBL) height 320 m was used in the first day. The initialization settings in the first day represented a horizontal advection bringing clean air above the SBL. For other

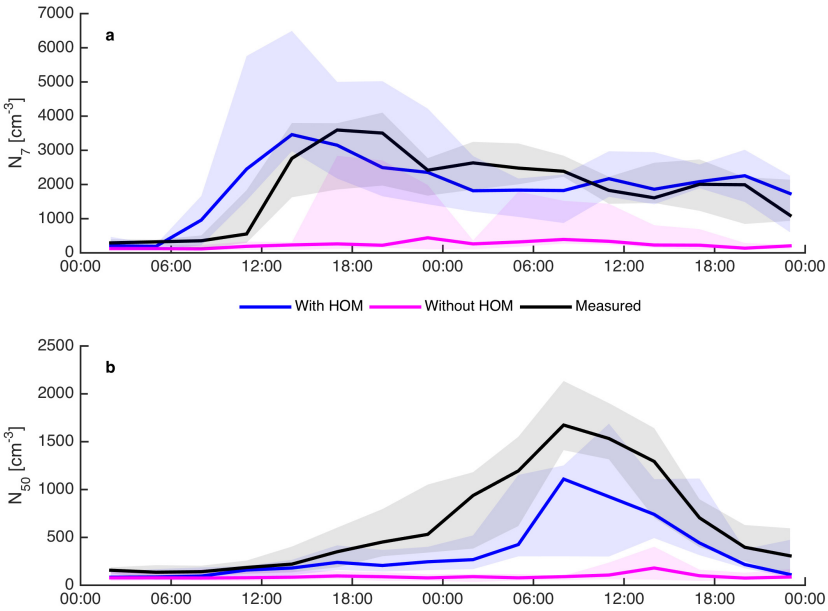

Figure 7: Modelled and measured (a) N_7 and (b) N_{50}. The model results are shown for simulations with or without HOM formation via autoxidation of monoterpenes. The solid lines show the median values from 10 NPF events at Pallas. The shaded areas give the 25% to 75% interval.

days, the nighttime residual layer was retained and the mixed layer (ML) growth in the morning would have less impact on vertical mixing of particles than the first day. Other model configurations were commonly used in SOSAA simulations (**Paper I**).

Figure 8 illustrates the simulated normalized exchange velocites for the first and second days (1 May and 2 May), one with NPF event and the other without. On the first day, the aerosol dynamics can be neglected because no NPF occurs (Fig. 8c). Therefore, the upward fluxes for 30, 100 and 300 nm sizes are mainly caused by the growth of ML which leads to the mixing of air with higher and lower particle concentrations (Figs. 8b and d). On the second day, when the NPF event starts, the storage term increases inside the canopy for 3, 10 and 30 nm sizes and decreases for 100 nm size

due to condensation growth of particles (Figs. 8b and c). However, the exchange velocity above the canopy is still mainly determined by deposition because the vertical transport is the main mechanism to compensate the particle loss due to deposition. But when the ML starts to grow and facilitate the vertical mixing, the concentration gradients established from the beginning of the NPF event finally lead to downward fluxes for 3, 10 and 30 nm sizes and upward flux for 100 nm size (Fig. 8d). The exchange velocities of 3, 10 and 30 nm sizes are several times as the deposition velocity (Fig. 8d), implying the dominant impact from aerosol dynamics. The simulation cases investigated in **Paper I** have verified the deviation of particle fluxes above the canopy from the dry deposition inside the forest. Moreover, this bias varies with the PBL development, particle size and the presence of NPF event.

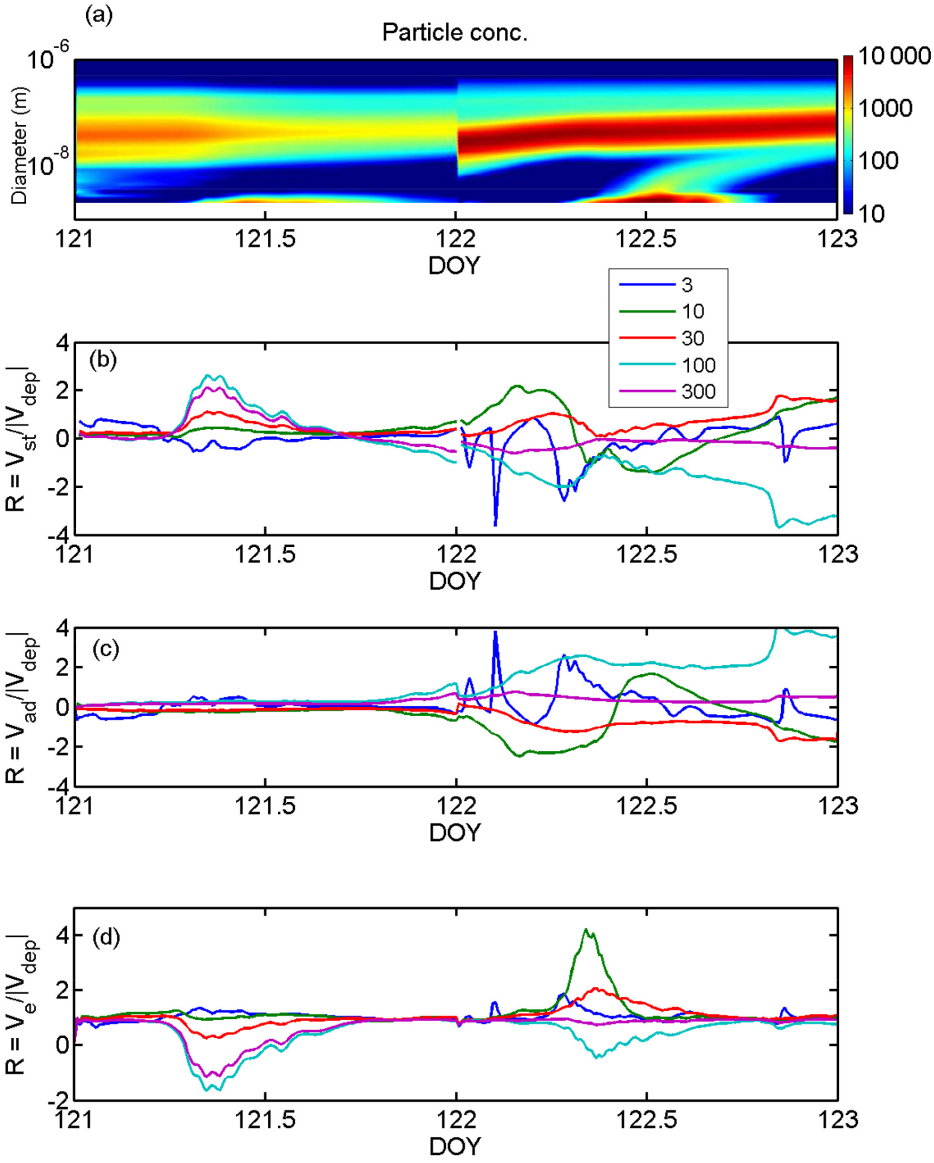

Figure 8: (a) Particle size spectrum and the exchange velocities (presented as the ratios to the absolute value of the deposition term) for selected particle sizes for (b) storage, (c) aerosol dynamics and (d) vertical exchange during 1 and 2 May (DOY 121 and 122) 2013. The discontinuity in midnight is due to the initialization of the particle size distribution every day. This figure is from Fig. 8 in **Paper I**.

4 Review of papers and the author's contribution

In **Paper I** we have analysed the impacts of aerosol dynamics and PBL development on the vertical transport of aerosol particles above a boreal forest canopy. It simulates a 10-day time period with frequent NPF events. The model results show that the aerosol dynamical processes regulate the particle number concentration throughout the whole PBL column. During the periods with strong aerosol dynamics, e.g., in a NPF event, the integrated particle number concentration tendency inside the canopy due to aerosol dynamics is comparable or exceeds that due to particle dry deposition. This indicates the measured particle fluxes above the canopy can deviate from the particle dry deposition sink inside the forest. The magnitude of this impact strongly depends on particle size and ABL development. I contributed to the algorithms of calculating particle deposition and aerosol fluxes in the model. I also contributed to writing the manuscript.

In **Paper II** we have analysed the measured fluxes of formic acid over a boreal forest. The observed high upward fluxes can not be explained by currently known chemical production mechanisms and emission rates. This implies missing chemical production from unknown precursors and unidentified emission sources. After adding an artificial emission source of formic acid in a global model to match the observed fluxes, the model biases against measurements are reduced in the PBL. However, the concentration is still underestimated in the free troposphere. I implemented the gas dry deposition model in SOSAA which was then used to calculate the chemical production of formic acid. I also contributed to the texts related to dry deposition in the manuscript.

In **Paper III** we implement a new O_3 dry deposition model into a 1D chemical transport model SOSAA. It models the O_3 deposition processes inside a boreal forest. The model results show that the wet skin uptake contributes $\sim 51\%$ to the total deposition at nighttime and $\sim 19\%$ at daytime when RH $> 70\%$. And the soil deposition contributes $\sim 36\%$. The O_3 concentration change due to air chemistry plays a minor role which is in average less than 10% of the dry deposition loss. I implemented the O_3 dry deposition model into SOSAA, did all the simulation runs and wrote most of the manusript.

In **Paper IV** we simulate 10 NPF events along their corresponding 7-day backward air mass trajectories with a Lagrangian model ADCHEM. HOMs can participate in particle formation and growth. The modelled mass fraction of HOMs in SOA is $\sim 75\%$.

The model predicts 2-hour earlier NPF event than observation and underestimates the number concentration of particles larger than 50 nm. The O:C ratio in the SOA is overestimated. All of these possibly result from less involvement of SVOCs on particle growth or missing production pathways of SVOCs. I supported the lead author in setting up the model for the Pallas field station, in the writing of the paper and implementation of the MCMv3.3.1 in ADCHEM.

In **Paper V** we extend the gas dry deposition model in SOSAA to calculate the dry deposition processes of them. It then models the in-canopy sources and sinks of 12 featured BVOCs. According to the significance of different sources and sinks, the BVOCs are classified into five categories: Cemis, Cchem-depo, Cemis-Cdepo, Cdepo, Cchem-depo. This classification is expected to be applicable in other ecosystems for other BVOCs. I implemented the gas dry deposition model into SOSAA, did all the simulation runs and wrote most of the manusript.

5 Conclusions

The sources, sinks and roles of BVOCs within and above the boreal forest canopy were investigated with two 1D numerical models in this thesis. The model simulations enabled us to separate individual processes which was not available only by analysing the measurement data. The main conclusions of this thesis are shown below.

In order to simulate detailed source and sink terms of BVOCs in a boreal forest, we implemented a new gas dry deposition model into the 1D chemical transport model SOSAA. It was first applied to simulate BVOC fluxes over a boreal forest canopy to testify its performance. By comparing the modelled and measured monthly-averaged diurnal variations of the fluxes of six BVOCs or groups of BVOCs, (monoterpenes, isoprene+MBO, methanol, acetaldehyde, acetone, formaldehyde), the model was proved to be able to predict well the source and sink terms of BVOCs (**Paper V**). However, with our currently known chemical mechanism and emission rates, the model failed to predict the high upward fluxes of formic acid which were measured from 28 April to 3 June 2014 over a pine forest at SMEAR II. We concluded that some precursors of formic acid and emission sources were still unidentified (**Paper II**).

We then selected 12 featured BVOCs at SMEAR II and analysed their in-canopy sources and sinks. Although there exist a huge amount of different BVOCs, they can be classified into limited categories according to the significance of their individual source and sink terms. In this thesis, we put them into five classes: Cemis in which the emitted gases are mostly transported out of the canopy (e.g., monoterpenes, isoprene+MBO), Cemis-chem in which the emitted gases are quickly oxidized inside the canopy (e.g., sesquiterpenes), Cemis-depo in which emission is comparable to deposition (e.g., acetaldehyde, methanol, acetone, formaldehyde, formic acid), Cdepo in which deposition sink dominates leading to prevalent downward fluxes (e.g., acetol, pinic acid, BCSOZOH) and Cchem-depo in which the chemical production can be comparable to deposition (e.g., ISOP34OOH, ISOP34NO3). This classification is expected to be valid in other ecosystems (**Paper V**).

The impact of BVOCs on the O_3 concentration change inside the canopy was also studied. Although at some specific time, the net chemical production and loss of O_3 mainly due to reactions with BVOCs could reach $\sim$ 20% of the deposition sink, the average contribution was less than 10%. Therefore, the air chemistry only plays a minor role in altering O_3 concentration inside the canopy (**Paper III**).

HOMs, as a portion of BVOCs if we do not consider anthropogenic VOCs in a boreal forest, can participate in particle formation and growth. Therefore, we quantified the role of HOMs in aerosol dynamics by simulating 10 NPF events along the 7-day backward air mass trajectories at Pallas which is a very remote site with very little anthropogenic impact. The model predicted the onset of NPF events about 2 hours earlier compared to observation. The number concentration of particles larger than 50 nm was underestimated, but the temporal pattern was similar with measurement. In addition, the modelled O:C ratio (0.99) was higher than the observed ratio (0.73). However, according to a recent revision suggested by Canagaratna et al. (2015), the observed O:C ratio should be 0.93 which is close to the modelled one. We proposed that using corrected saturation vapor pressure of HOMs and increasing the involvement of SVOCs in particle growth could improve the model performance. With the current model configuration, HOMs were found to constitue $\sim$ 75% of the total SOA mass (**Paper IV**).

HOMs play a dominant role in the aerosol dynamics, which spans about 3 orders of magnitude of timescales from half an hour to tens of hours depending on particles sizes. The aerosol dynamics was found to impact the aerosol fluxes above the canopy during the NPF events. This could deviate the measured aerosol flux from deposition flux which complicates the interpretation of the aerosol vertical transport. The model results showed that the impact of aerosol on this deviation strongly depended on particle size and PBL development (**Paper I**).

In conclusion, the answers to the main objectives of this thesis are summarised below:

1. In **Paper V**, we quantified the relative contributions of emissions, chemical reactions, dry deposition and turbulent transport for 12 featured BVOCs within a boreal forest at SMEAR II with the newly implemented gas dry deposition model, which are shown in Fig. 4. The fluxes of monoterpenes, isoprene+MBO, methanol, acetaldehyde, acetone and formaldehyde at the canopy top were also simulated, which agreed well with the observation data. In **Paper II**, we analysed both the measured fluxes at the canopy top and the simulated in-canopy sources and sinks of formic acid at SMEAR II. The results implied that unidentified emission sources and chemical mechanisms were needed to explain the high upward fluxes.

2. In **Paper III**, we found that the average contribution of chemical reactions to

the in-canopy O_3 concentration tendency in August at SMEAR II was less than 10% of the dry depostion contribution (Fig. 6).

3. In **Paper IV**, the model results showed that the HOMs played a significant role in both particle formation and growth, which contributed about 75% of the total SOA mass during the NPF events at Pallas.

4. In **Paper I**, the model results showed that the aerosol dynamics significantly impacted the exchange velocites of aerosol particles at the canopy top at SMEAR II, which deviated the aerosol fluxes from deposition fluxes by up to 4 times (Fig. 8).

In this thesis we have provided an insight into the fate of BVOCs from production to removal and from gas phase to particle phase. However, the model is always far from perfect, it should be improved as more measurement data are available. For example, the measurement data of BVOC fluxes are still scarce, especially for the reactive ones, this will introduce large biases in the emission and deposition models. In future, the work in this thesis can be extended from near the canopy to larger scales incorporating the PBL and the 3D heterogeneity of the forest areas. The interactions with clouds can also be included to make a real closure of a BVOC life.

References

Altimir, N., Kolari, P., Tuovinen, J.-P., Vesala, T., Bäck, J., Suni, T., Kulmala, M., and Hari, P. (2006). Foliage surface ozone deposition: a role for surface moisture? *Biogeosciences*, 3:209–228.

Ashworth, K., Chung, S. H., Griffin, R. J., Chen, J., Forkel, R., Bryan, A. M., and Steiner, A. L. (2015). FORest Canopy Atmosphere Transfer (FORCAsT) 1.0: a 1-D model of biosphere-atmosphere chemical exchange. *Geoscientific Model Development*, 8(11):3765–3784.

Atkinson, R. (1997). Gas-Phase Tropospheric Chemistry of Volatile Organic Compounds: 1. Alkanes and Alkenes. *Journal of Physical and Chemical Reference Data*, 26(2):215–290.

Bäck, J., Aalto, J., Henriksson, M., Hakola, H., He, Q., and Boy, M. (2012). Chemodiversity of a Scots pine stand and implications for terpene air concentrations. *Biogeosciences*, 9:689–702.

Beecken, J., Mellqvist, J., Salo, K., Ekholm, J., Jalkanen, J.-P., Johansson, L., Litvinenko, V., Volodin, K., and Frank-Kamenetsky, D. A. (2015). Emission factors of SO_2, NO_x and particles from ships in Neva Bay from ground-based and helicopter-borne measurements and AIS-based modeling. *Atmospheric Chemistry and Physics*, 15(9):5229–5241.

Boy, M., Mogensen, D., Smolander, S., Zhou, L., Nieminen, T., Paasonen, P., Plass-Dülmer, C., Sipilä, M., Petäjä, T., Mauldin, L., Berresheim, H., and Kulmala, M. (2013). Oxidation of SO_2 by stabilized Criegee intermediate (sCI) radicals as a crucial source for atmospheric sulfuric acid concentrations. *Atmospheric Chemistry and Physics*, 13(7):3865–3879.

Boy, M., Sogachev, A., Lauros, J., Zhou, L., Guenther, A., and Smolander, S. (2011). SOSA–a new model to simulate the concentrations of organic vapours and sulphuric acid inside the ABL – Part 1: Model description and initial evaluation. *Atmos. Chem. Phys.*, 11:43–51.

Canagaratna, M. R., Jimenez, J. L., Kroll, J. H., Chen, Q., Kessler, S. H., Massoli, P., Hildebrandt Ruiz, L., Fortner, E., Williams, L. R., Wilson, K. R., Surratt, J. D., Donahue, N. M., Jayne, J. T., and Worsnop, D. R. (2015). Elemental ratio

measurements of organic compounds using aerosol mass spectrometry: characterization, improved calibration, and implications. *Atmospheric Chemistry and Physics*, 15(1):253–272.

Damian, V., Sandu, A., Damian, M., Potra, F., and Carmichael, G. R. (2002). The kinetic preprocessor KPP-a software environment for solving chemical kinetics. *Computers & Chemical Engineering*, 26(11):1567 – 1579.

Dee, D. P., Uppala, S. M., Simmons, A. J., Berrisford, P., Poli, P., Kobayashi, S., Andrae, U., Balmaseda, M. A., Balsamo, G., Bauer, P., Bechtold, P., Beljaars, A. C. M., van de Berg, L., Bidlot, J., Bormann, N., Delsol, C., Dragani, R., Fuentes, M., Geer, A. J., Haimberger, L., Healy, S. B., Hersbach, H., Hólm, E. V., Isaksen, L., Kållberg, P., Köhler, M., Matricardi, M., McNally, A. P., Monge-Sanz, B. M., Morcrette, J.-J., Park, B.-K., Peubey, C., de Rosnay, P., Tavolato, C., Thépaut, J.-N., and Vitart, F. (2011). The era-interim reanalysis: configuration and performance of the data assimilation system. *Quarterly Journal of the Royal Meteorological Society*, 137(656):553–597.

Ehn, M., Thornton, J. A., Kleist, E., Sipilä, M., Junninen, H., Pullinen, I., Springer, M., Rubach, F., Tillmann, R., Lee, B., Lopez-Hilfiker, F., Andres, S., Acir, I.-H., Rissanen, M., Jokinen, T., Schobesberger, S., Kangasluoma, J., Kontkanen, J., Nieminen, T., Kurtén, T., Nielsen, L. B., Jørgensen, S., Kjaergaard, H. G., Canagaratna, M., Maso, M. D., Berndt, T., Petäjä, T., Wahner, A., Kerminen, V.-M., Kulmala, M., Worsnop, D. R., Wildt, J., and Mentel, T. F. (2014). A large source of low-volatility secondary organic aerosol. *Nature*, 506:476.

Felzer, B. S., Cronin, T., Reilly, J. M., Melillo, J. M., and Wang, X. (2007). Impacts of ozone on trees and crops. *Comptes Rendus Geoscience*, 339:784–798.

Ganzeveld, L. and Lelieveld, J. (1995). Dry deposition parameterization in a chemistry general circulation model and its influence on the distribution of reactive trace gases. *J. Geophy. Res.*, 100:20999–21012.

Ganzeveld, L., Lelieveld, J., and Roelofs, G.-J. (1998). A dry deposition parameterization for sulfur oxides in a chemistry and general circulation model. *Journal of Geophysical Research: Atmospheres*, 103(D5):5679–5694.

Ganzeveld, L. N., Lelieveld, J., Dentener, F. J., Krol, M. C., and Roelofs, G.-J. (2002).

Atmosphere-biosphere trace gas exchanges simulated with a single-column model. *Journal of Geophysical Research*, 107(D16):ACH 8–1–ACH 8–21.

Goldstein, A. H. and Galbally, I. E. (2007). Known and unexplored organic constituents in the earth's atmosphere. *Environmental Science & Technology*, 41(5):1514–1521. PMID: 17396635.

Guenther, A. B., Jiang, X., Heald, C. L., Sakulyanontvittaya, T., Duhl, T., Emmons, L. K., and Wang, X. (2012). The Model of Emissions of Gases and Aerosols from Nature version 2.1 (MEGAN2.1): an extended and updated framework for modeling biogenic emissions. *Geosci. Model Dev.*, 5:1471–1492.

Guenther, A. B., Karl, T., Harley, P., Wiedinmyer, C., Palmer, P. I., and Geron, C. (2006). Estimates of global terrestrial isoprene emissions using MEGAN(Model of Emissions of Gases and Aerosols from Nature). *Atmos. Chem. Phys.*, 6:3181–3210.

Haapanala, S., Rinne, J., Hakola, H., Hellén, H., Laakso, L., Lihavainen, H., Janson, R., O'Dowd, C., and Kulmala, M. (2007). Boundary layer concentrations and landscape scale emissions of volatile organic compounds in early spring. *Atmos. Chem. Phys.*, 7:1869–1878.

Hari, P. and Kulmala, M. (2005). Station for measuring ecosystem-atmosphere relations (smear ii). *Boreal. Environ. Res.*, 10:315–322.

Hine, J. and Mookerjee, P. K. (1975). Structural effects on rates and equilibriums. XIX. Intrinsic hydrophilic character of organic compounds. correlations in terms of structural contributions. *The Journal of Organic Chemistry*, 40(3):292–298.

Ilvesniemi, H., Pumpanen, J., Duursma, R., Hari, P., Keronen, P., Kolari, P., Kulmala, M., Mammarella, I., Nikinmaa, E., Rannik, Ü., Pohja, T., Siivola, E., and Vesala, T. (2010). Water balance of a boreal scots pine forest. *Boreal Env. Res.*, 15:375–396.

Jaatinen, A., Romakkaniemi, S., Anttila, T., Hyvärinen, A.-P., Hao, L. Q., Kortelainen, A., Miettinen, P., Mikkonen, S., Smith, J. N., Virtanen, A., and Laaksonen, A. (2014). The third Pallas Cloud Experiment: Consistency between the aerosol hygroscopic growth and CCN activity. *Boreal Env. Res.*, 19:368 – 382.

Jenkin, M. E., Saunders, S. M., and Pilling, M. J. (1997). The tropospheric degradation of volatile organic compounds: a protocol for mechanism development. *Atmospheric Environment*, 31(1):81 – 104.

Jenkin, M. E., Wyche, K. P., Evans, C. J., Carr, T., Monks, P. S., Alfarra, M. R., Barley, M. H., McFiggans, G. B., Young, J. C., and Rickard, A. R. (2012). Development and chamber evaluation of the MCM v3.2 degradation scheme for β-caryophyllene. *Atmospheric Chemistry and Physics*, 12(11):5275–5308.

Jimenez, J. L., Canagaratna, M. R., Donahue, N. M., Prevot, A. S. H., Zhang, Q., Kroll, J. H., DeCarlo, P. F., Allan, J. D., Coe, H., Ng, N. L., Aiken, A. C., Docherty, K. S., Ulbrich, I. M., Grieshop, A. P., Robinson, A. L., Duplissy, J., Smith, J. D., Wilson, K. R., Lanz, V. A., Hueglin, C., Sun, Y. L., Tian, J., Laaksonen, A., Raatikainen, T., Rautiainen, J., Vaattovaara, P., Ehn, M., Kulmala, M., Tomlinson, J. M., Collins, D. R., Cubison, M. J., Dunlea, J., Huffman, J. A., Onasch, T. B., Alfarra, M. R., Williams, P. I., Bower, K., Kondo, Y., Schneider, J., Drewnick, F., Borrmann, S., Weimer, S., Demerjian, K., Salcedo, D., Cottrell, L., Griffin, R., Takami, A., Miyoshi, T., Hatakeyama, S., Shimono, A., Sun, J. Y., Zhang, Y. M., Dzepina, K., Kimmel, J. R., Sueper, D., Jayne, J. T., Herndon, S. C., Trimborn, A. M., Williams, L. R., Wood, E. C., Middlebrook, A. M., Kolb, C. E., Baltensperger, U., and Worsnop, D. R. (2009). Evolution of organic aerosols in the atmosphere. *Science*, 326(5959):1525–1529.

Jokinen, T., Berndt, T., Makkonen, R., Kerminen, V.-M., Junninen, H., Paasonen, P., Stratmann, F., Herrmann, H., Guenther, A. B., Worsnop, D. R., Kulmala, M., Ehn, M., and Sipilä, M. (2015). Production of extremely low volatile organic compounds from biogenic emissions: Measured yields and atmospheric implications. *Proceedings of the National Academy of Sciences*, 112(23):7123–7128.

Junninen, H., Lauri, A., Keronen, P., Aalto, P., Hiltunen, V., Hari, P., and Kulmala, M. (2009). Smart-smear: on-line data exploration and visualization tool for smear stations. *Boreal Environment Research*, 14:447–457.

Kampa, M. and Castanas, E. (2008). Human health effects of air pollution. *Environmental Pollution*, 151:362–367.

Karl, T., Harley, P., Emmons, L., Thornton, B., Guenther, A., Basu, C., Turnipseed, A., and Jardine, K. (2010). Efficient atmospheric cleansing of oxidized organic trace gases by vegetation. *Science*, 330:816–819.

Kerminen, V.-M., Paramonov, M., Anttila, T., Riipinen, I., Fountoukis, C., Korhonen, H., Asmi, E., Laakso, L., Lihavainen, H., Swietlicki, E., Svenningsson, B., Asmi,

A., Pandis, S. N., Kulmala, M., and Petäjä, T. (2012). Cloud condensation nuclei production associated with atmospheric nucleation: a synthesis based on existing literature and new results. *Atmospheric Chemistry and Physics*, 12(24):12037–12059.

Kivekäs, N., Kerminen, V.-M., Raatikainen, T., Vaattovaara, P., Laaksonen, A., and Lihavainen, H. (2009). Physical and chemical characteristics of aerosol particles and cloud-droplet activation during the Second Pallas Cloud Experiment (Second PaCE). *Boreal Env. Res.*, 14:515 – 526.

Knote, C., Hodzic, A., and Jimenez, J. L. (2015). The effect of dry and wet deposition of condensable vapors on secondary organic aerosols concentrations over the continental us. *Atmospheric Chemistry and Physics*, 15(1):1–18.

Korhonen, H., Lehtinen, K. E. J., and Kulmala, M. (2004). Multicomponent aerosol dynamics model uhma: model development and validation. *Atmospheric Chemistry and Physics*, 4(3):757–771.

Kristensson, A., Johansson, C., Westerholm, R., Swietlicki, E., Gidhagen, L., Wideqvist, U., and Vesely, V. (2004). Real-world traffic emission factors of gases and particles measured in a road tunnel in Stockholm, Sweden. *Atmospheric Environment*, 38(5):657 – 673.

Kuhn, U., Rottenberger, S., Biesenthal, T., Ammann, C., Wolf, A., Schebeske, G., Oliva, S. T., Tavares, T. M., and Kesselmeier, J. (2002). Exchange of short-chain monocarboxylic acids by vegetation at a remote tropical forest site in Amazonia. *Journal of Geophysical Research: Atmospheres*, 107(D20):LBA 36–1–LBA 36–18. 8069.

Kulmala, M., Kontkanen, J., Junninen, H., Lehtipalo, K., Manninen, H. E., Nieminen, T., Petäjä, T., Sipilä, M., Schobesberger, S., Rantala, P., Franchin, A., Jokinen, T., Järvinen, E., Äijälä, M., Kangasluoma, J., Hakala, J., Aalto, P. P., Paasonen, P., Mikkilä, J., Vanhanen, J., Aalto, J., Hakola, H., Makkonen, U., Ruuskanen, T., Mauldin, R. L., Duplissy, J., Vehkamäki, H., Bäck, J., Kortelainen, A., Riipinen, I., Kurtén, T., Johnston, M. V., Smith, J. N., Ehn, M., Mentel, T. F., Lehtinen, K. E. J., Laaksonen, A., Kerminen, V.-M., and Worsnop, D. R. (2013). Direct observations of atmospheric aerosol nucleation. *Science*, 339(6122):943–946.

Kulmala, M., Maso, M. D., Mäkelä, J. M., Pirjola, L., Väkevä, M., Aalto, P., Miikkulainen, P., Hämeri, K., and O'dowd, C. D. (2001). On the formation, growth and composition of nucleation mode particles. *Tellus B*, 53(4):479–490.

Kurtén, T., Zhou, L., Makkonen, R., Merikanto, J., Räisänen, P., Boy, M., Richards, N., Rap, A., Smolander, S., Sogachev, A., Guenther, A., Mann, G. W., Carslaw, K., and Kulmala, M. (2011). Large methane releases lead to strong aerosol forcing and reduced cloudiness. *Atmospheric Chemistry and Physics*, 11(14):6961–6969.

Lammel, G. (1999). Formation of nitrous acid: parameterisation and comparison with observations. Technical Report REPORT No. 286, Max-Planck-Institut für Meteorologie.

Launiainen, S., Katul, G. G., Grönholm, T., and Vesala, T. (2013). Partitioning ozone fluxes between canopy and forest floor by measurements and a multi-layer model. *Agricultural and Forest Meteorology*, 173:85–99.

Lee, B. H., Lopez-Hilfiker, F. D., Mohr, C., Kurtén, T., Worsnop, D. R., and Thornton, J. A. (2014). An iodide-adduct high-resolution time-of-flight chemical-ionization mass spectrometer: Application to atmospheric inorganic and organic compounds. *Environmental Science & Technology*, 48(11):6309–6317. PMID: 24800638.

Lohila, A., Penttilä, T., Jortikka, S., Aalto, T., Anttila, P., Asmi, E., M., A., Hatakka, J., Hellén, H., H., H., Hänninen, P., Kilkki, J., Kyllönen, K., Laurila, T., Lepistö, A., Lihavainen, H., Makkonen, U., Paatero, J., Rask, M., Sutinen, R., Tuovinen, J.-P., Vuorenmaa, J., and Viisanen, Y. (2015). Preface to the special issue on integrated research of atmosphere, ecosystems and environment at Pallas. *Boreal Env. Res.*, 20:431–454.

Mårtensson, E. M., Nilsson, E. D., de Leeuw, G., Cohen, L. H., and Hansson, H.-C. (2003). Laboratory simulations and parameterization of the primary marine aerosol production. *Journal of Geophysical Research: Atmospheres*, 108(D9):n/a–n/a. 4297.

Meyers, T. P. (1987). The sensitivity of modeled SO_2 fluxes and profiles to stomatal and boundary layer resistances. *Water, Air, and Soil Pollution*, 35(3):261–278.

Meylan, W. M. and Howard, P. H. (1991). Bond contribution method for estimating henry's law constants. *Environmental Toxicology and Chemistry*, 10(10):1283–1293.

Mogensen, D., Gierens, R., Crowley, J. N., Keronen, P., Smolander, S., Sogachev, A., Nölscher, A. C., Zhou, L., Kulmala, M., Tang, M. J., Williams, J., and Boy, M. (2015). Simulations of atmospheric OH, O_3 and NO_3 reactivities within and above the boreal forest. *Atmos. Chem. Phys.*, 15:3909–3932.

Mogensen, D., Smolander, S., Sogachev, A., Zhou, L., Sinha, V., Guenther, A., Williams, J., Nieminen, T., Kajos, M. K., Rinne, J., Kulmala, M., and Boy, M. (2011). Modelling atmospheric OH-reactivity in a boreal forest ecosystem. *Atmos. Chem. Phys.*, 11:9709–9719.

Nemitz, E., Sutton, M. A., Schjoerring, J. K., Husted, S., and Paul, W. G. (2000). Resistance modelling of ammonia exchange over oilseed rape. *Agricultural and Forest Meteorology*, 105:405–425.

Ng, N. L., Canagaratna, M. R., Zhang, Q., Jimenez, J. L., Tian, J., Ulbrich, I. M., Kroll, J. H., Docherty, K. S., Chhabra, P. S., Bahreini, R., Murphy, S. M., Seinfeld, J. H., Hildebrandt, L., Donahue, N. M., DeCarlo, P. F., Lanz, V. A., Prévôt, A. S. H., Dinar, E., Rudich, Y., and Worsnop, D. R. (2010). Organic aerosol components observed in northern hemispheric datasets from aerosol mass spectrometry. *Atmospheric Chemistry and Physics*, 10(10):4625–4641.

Nguyen, T. B., Crounse, J. D., Teng, A. P., St. Clair, J. M., Paulot, F., Wolfe, G. M., and Wennberg, P. O. (2015). Rapid deposition of oxidized biogenic compounds to a temperate forest. *PNAS*, 112(5):E392–E401.

Niinemets, Ü., Fares, S., Harley, P., and Jardine, K. J. (2014). Bidirectional exchange of biogenic volatiles with vegetation: emission sources, reactions, breakdown and deposition. *Plant, Cell & Environment*, 37(8):1790–1809.

Pirjola, L., Kulmala, M., Wilck, M., Bischoff, A., Stratmann, F., and Otto, E. (1999). Formation of sulphuric acid aerosols and cloud condensation nuclei: an expression for significant nucleation and model comprarison. *Journal of Aerosol Science*, 30(8):1079 – 1094.

Pryor, S. C. and Binkowski, F. S. (2004). An analysis of the time scales associated with aerosol processes during dry deposition. *Aerosol Sci. Tech.*, 38:1091–1098.

Pumpanen, J., Ilvesniemi, H., Perämäki, M., and Hari, P. (2003). Seasonal patterns of soil CO_2 efflux and soil air CO_2 concentration in a Scots pine forest: comparison of two chamber techniques. *Global Change Biology*, 9(3):371–382.

Rannik, Ü. (1998). On the surface layer similarity at a complex forest site. *Journal of Geophysical Research: Atmospheres*, 103(D8):8685–8697.

Rannik, U., Altimir, N., Mammarella, I., Bäck, J., Rinne, J., Ruuskanen, T. M., Hari, P., Vesala, T., and Kulmala, M. (2012). Ozone deposition into a boreal forest over a decade of observations: evaluating deposition partitioning and driving variables. *Atmospheric Chemistry and Physics*, 12(24):12165–12182.

Rantala, P., Aalto, J., Taipale, R., Ruuskanen, T. M., and Rinne, J. (2015). Annual cycle of volatile organic compound exchange between a boreal pine forest and the atmosphere. *Biogeosciences*, 12(19):5753–5770.

Rantala, P., Taipale, R., Aalto, J., Kajos, M. K., Patokoski, J., Ruuskanen, T. M., and Rinne, J. (2014). Continuous flux measurements of VOCs using PTR-MS - reliability and feasibility of disjunct-eddy-covariance, surface-layer-gradient, and surface-layer-profile methods. *Boreal Environment Research*, 19:87–107.

Rinne, J., Bäck, J., and Hakola, H. (2009). Biogenic volatile organic compound emissions from the eurasian taiga: current knowledge and future directions. *Boreal Environment Research*, 14:807–826.

Roldin, P., Liao, L., Mogensen, D., Dal Maso, M., Rusanen, A., Kerminen, V.-M., Mentel, T. F., Wildt, J., Kleist, E., Kiendler-Scharr, A., Tillmann, R., Ehn, M., Kulmala, M., and Boy, M. (2015). Modelling the contribution of biogenic volatile organic compounds to new particle formation in the jülich plant atmosphere chamber. *Atmospheric Chemistry and Physics*, 15(18):10777–10798.

Roldin, P., Swietlicki, E., Schurgers, G., Arneth, A., Lehtinen, K. E. J., Boy, M., and Kulmala, M. (2011). Development and evaluation of the aerosol dynamics and gas phase chemistry model adchem. *Atmospheric Chemistry and Physics*, 11(12):5867–5896.

Rolph, G., Stein, A., and Stunder, B. (2017). Real-time Environmental Applications and Display sYstem: READY. *Environmental Modelling & Software*, 95(Supplement C):210 – 228.

Ruckstuhl, K. E., Johnson, E. A., and Miyanishi, K. (2008). Introduction. the boreal forest and global change. *Philosophical Transactions of the Royal Society of London B: Biological Sciences*, 363(1501):2243–2247.

Sander, R. (2015). Compilation of Henry's law constants (version 4.0) for water as solvent. *Atmospheric Chemistry and Physics*, 15:4399–4981.

Saunders, S. M., Jenkin, M. E., Derwent, R. G., and Pilling, M. J. (2003). Protocol for the development of the Master Chemical Mechanism, MCM v3 (Part A): tropospheric degradation of non-aromatic volatile organic compounds. *Atmospheric Chemistry and Physics*, 3(1):161–180.

Schallhart, S., Rantala, P., Nemitz, E., Taipale, D., Tillmann, R., Mentel, T. F., Loubet, B., Gerosa, G., Finco, A., Rinne, J., and Ruuskanen, T. M. (2016). Characterization of total ecosystem-scale biogenic voc exchange at a mediterranean oak–hornbeam forest. *Atmospheric Chemistry and Physics*, 16(11):7171–7194.

Smith, B., Wårlind, D., Arneth, A., Hickler, T., Leadley, P., Siltberg, J., and Zaehle, S. (2014). Implications of incorporating n cycling and n limitations on primary production in an individual-based dynamic vegetation model. *Biogeosciences*, 11(7):2027–2054.

Smolander, S., He, Q., Mogensen, D., Zhou, L., Bäck, J., Ruuskanen, T., Noe, S., Guenther, A., Aaltonen, H., Kulmala, M., and Boy, M. (2014). Comparing three vegetation monoterpene emission models to measured gas concentrations with a model of meteorology, air chemistry and chemical transport. *Biogeosciences*, 11:5425–5443.

Sogachev, A., Menzhulin, G., Heimannn, M., and Lloyd, J. (2002). A simple three dimensional canopy – planetary boundary layer simulation model for scalar concentrations and fluxes. *Tellus*, 54B:784–819.

Spracklen, D. V., Bonn, B., and Carslaw, K. S. (2008). Boreal forests, aerosols and the impacts on clouds and climate. *Philosophical Transactions of the Royal Society of London A: Mathematical, Physical and Engineering Sciences*, 366(1885):4613–4626.

Stein, A. F., Draxler, R. R., Rolph, G. D., Stunder, B. J. B., Cohen, M. D., and Ngan, F. (2015). NOAA's HYSPLIT Atmospheric Transport and Dispersion Modeling System. *Bulletin of the American Meteorological Society*, 96(12):2059–2077.

Stocker, T. F., Qin, D., Plattner, G.-K., Tignor, M., Allen, S. K., Boschung, J., Nauels, A., Xia, Y., Bex, V., and Midgley, P. M. (2013). *IPCC, 2013: Climate Change 2013: The Physical Science Basis. Contribution of Working Group I to the Fifth Assessment Report of the Intergovernmental Panel on Climate Change*. Cambridge University Press, Cambridge, United Kingdom and New York, NY, USA.

Tröstl, J., Chuang, W. K., Gordon Hamish, Heinritzi Martin, Yan Chao, Molteni Ugo, Ahlm Lars, Frege Carla, Bianchi Federico, Wagner Robert, Simon Mario, Lehtipalo Katrianne, Williamson Christina, Craven Jill S., Duplissy Jonathan, Adamov Alexey, Almeida Joao, Bernhammer Anne-Kathrin, Breitenlechner Martin, Brilke Sophia, Dias António, Ehrhart Sebastian, Flagan Richard C., Franchin Alessandro, Fuchs Claudia, Guida Roberto, Gysel Martin, Hansel Armin, Hoyle Christopher R., Jokinen Tuija, Junninen Heikki, Kangasluoma Juha, Keskinen Helmi, Kim Jaeseok, Krapf Manuel, Kürten Andreas, Laaksonen Ari, Lawler Michael, Leiminger Markus, Mathot Serge, Möhler Ottmar, Nieminen Tuomo, Onnela Antti, Petäjä Tuukka, Piel Felix M., Miettinen Pasi, Rissanen Matti P., Rondo Linda, Sarnela Nina, Schobesberger Siegfried, Sengupta Kamalika, Sipilä Mikko, Smith James N., Steiner Gerhard, Tomé António, Virtanen Annele, Wagner Andrea C., Weingartner Ernest, Wimmer Daniela, Winkler Paul M., Ye Penglin, Carslaw Kenneth S., Curtius Joachim, Dommen Josef, Kirkby Jasper, Kulmala Markku, Riipinen Ilona, Worsnop Douglas R., Donahue Neil M., and Baltensperger Urs (2016). The role of low-volatility organic compounds in initial particle growth in the atmosphere. *Nature*, 533:527.

US EPA (2017). Estimation programs interface suite™ for microsoft® windows, v 4.11.

Wesely, M. L. (1989). Parameterization of surface resistances to gaseous dry deposition in regional-scale numerical models. *Atmos. Env.*, 23:1293–1304.

Wolfe, G. M., Thornton, J. A., McKay, M., and Goldstein, A. H. (2011). Forest-atmosphere exchange of ozone: sensitivity to very reactive biogenic voc emissions and implications for in-canopy photochemistry. *Atmospheric Chemistry and Physics*, 11(15):7875–7891.

Wu, Y., Brashers, B., Finkelstein, P. L., and E., P. J. (2003). A multilayer biochemical dry deposition model 1. model formulation. *Journal of Geophysical Research: Atmospheres*, 108(D1).

Zhang, L., Brook, J. R., and Vet, R. (2003). A revised parameterization for gaseous dry deposition in air-quality models. *Atmospheric Chemistry and Physics*, 3(6):2067–2082.

Zhou, L., Nieminen, T., Mogensen, D., Smolander, S., Rusanen, A., Kulmala, M., and Boy, M. (2014). SOSAA – a new model to simulate the concentrations of organic

vapours, sulphuric acid and aerosols inside the ABL – Part 2: Aerosol dynamics and one case study at a boreal forest site. *Boreal Environment Research*, 19 (suppl. B):237–256.